

Isolation of two putative homologues of *PISTILLATA* and *AGAMOUS* from *Alpinia oblongifolia* (Zingiberaceae) and characterization of their expression

Xue-Mei Gao, Yong-Mei Xia, Qing-Jun Li*

Xishuangbanna Tropical Botanical Garden, Chinese Academy of Sciences, Yunnan 666303, China

Received 28 June 2005; received in revised form 20 October 2005; accepted 1 November 2005

Available online 28 November 2005

Abstract

We cloned the cDNAs of AG- and PI-like genes from a young inflorescence cDNA library of *Alpinia oblongifolia*. Two MADS-box related clones were repeatedly isolated: *A. oblongifolia PISTILLATA* (*AoPI*) and *A. oblongifolia AGAMOUS* (*AoAG*). *AoPI* cDNA is 841 bp long including the poly-A tail instead of 826 bp long and encodes a 208 amino acid peptide. *AoAG* is 971 bp long and encodes a 229 amino acid peptide. Sequence comparisons indicated that *AoPI* and *AoAG* are very similar to *PI* and *AG* homologues, respectively. Phylogenetic analyses showed that *AoPI* belongs to the *PI* group and *AoAG* belongs to the *AG* group of genes. In situ hybridization demonstrated that the *AoPI* gene is expressed in petals and stamen throughout the process of flower development, and that the *AoAG* gene is expressed in stamen throughout flower development and in carpels in the early stages of development. *AoAG* is also expressed in the ovules. The expression patterns of *AoPI* and *AoAG* are generally consistent with those of the floral homeotic *PI*- and *AG*-like genes in other plant species; these specify the identities of the second and third whorls, and third and fourth whorls, respectively. Therefore, in *A. oblongifolia*, *AoPI* is a B-functional gene and *AoAG* is a C-functional gene. The conservation and diversification of the expression of both genes are discussed.

© 2005 Elsevier Ireland Ltd. All rights reserved.

Keywords: MADS-box; ABC model; *AoPI*; *AoAG*; Floral development; Flexistyl

1. Introduction

Flowers are a defining characteristic of angiosperms and show enormous morphological diversity. However, the fundamental floral architecture is conserved. A typical hermaphroditic flower contains stamens and carpels, which are surrounded by sterile perianth organs [1,2]. These organs are generally arranged into whorls. The first and second whorls of a flower contain the sterile sepals and petals, respectively. The third whorl contains stamens, the male reproductive structures that produce pollen. The female reproductive structures, the carpels, constitute the fourth whorl and contain the ovules [2]. Although there are many differences in floral morphology and function in different plants, the genetic mechanisms regulating the ontogeny of flowers are relatively conserved. Some conserved transcription factors interact to determine the identities and relative positions of the floral organs [3].

Floral organ identity genes are important developmental genes that control flower formation. These factors have been identified by genetic analyses of floral homeotic mutants in the model species *Arabidopsis thaliana* [4] and *Antirrhinum majus* [5]. In the well-known “ABC model”, three classes of floral organ identity genes, A, B, and C, specify the identities of different floral organs. These act in combination, with A specifying the sepals in the first floral whorl, A + B the petals in the second whorl, B + C the stamens in the third whorl, and C the carpels in the fourth whorl [6,7]. Based on studies in petunia (*Petunia hybrida*), the ABC model has been extended to include class D genes, which specify the development of ovules [8]. It has also been demonstrated with a reverse-genetic approach that yet another class of floral organ identity genes, class E or *SEPALLATA* genes, is involved in specifying the development of petals, stamens, and carpels [2,9,10]. The ABC model has thus been extended to the ABCDE model, with A specifying sepals, A + B + E petals, B + C + E stamens, C + E carpels, and D ovules [2].

In *Arabidopsis*, class A genes comprise *APETALA1* (*AP1*) and *APETALA2* (*AP2*) [11,12], and class B genes are represented by *APETALA3* (*AP3*) and *PISTILLATA* (*PI*)

* Corresponding author. Tel.: +86 691 8715471; fax: +86 691 8715070.

E-mail address: qjlixtbg@bn.yn.cninfo.net (Q.-J. Li).

[13,14]. The class C gene is *AGAMOUS* (*AG*) [15], and the class D gene is *AGL11* [2]. Class E genes comprise *SEPALLATA1* (*SEP1*), *SEPALLATA2* (*SEP2*), and *SEPALLATA3* (*SEP3*), all of which have highly redundant functions [9,10].

Although much is known about the functions of the ABC gene products in dicots, those in monocots have only been reported in a few species, including rice [16], maize [17], and wheat [18], all of which belong to the grass family (Poaceae).

OsMADS18 from rice (*Oryza sativa*) belongs to the phylogenetically defined *API/SQUA* group, the overexpression of which induces early flowering. The overexpression of *OsMADS18* in *Arabidopsis* causes a phenotype closely resembling the *ap1* mutant [19]. In rice, two *PI* group genes, *OsMADS2* and *OsMADS4*, were isolated [20]. They show expression patterns similar to those of the class B genes in *Arabidopsis*. Transgenic rice plants expressing anti-sense *OsMADS4* displayed alterations in the second and third whorls [21]. Second-whorl lodicules were altered to palea/lemma-like organs, and third-whorl stamens were changed to carpel-like organs. These results suggest that *OsMADS4* belongs to the *PI* gene group. Loss of function of the *DEF*-like gene *SILKY1* in maize results in homeotic transformations of the lodicules into palea/lemma-like organs, and transformation of the stamens into carpelloid organs [22]. It has been proposed that the C-function gene in *O. sativa* is *OsMADS3* [23]. In maize, the C-function gene is regulated by two closely related *AG* homologues, *ZAG1* and *ZMM2* [24].

This suggests that the ABC model might also be applicable to grasses, except that the palea and lemma are sepal homologues specified by A-function genes and the lodicules are homologous petal organs specified by a combination of A- and B-function genes [21,22]. In both monocots and eudicots, B and C functions require genes homologous to *AP3*, *PI*, and *AG*, indicating a high degree of evolutionary conservation in this regulatory system among angiosperms [2].

Other than *AP2*, all floral organ identity genes belong to the family of MADS-box genes, which encode transcription factors [2,7,25,26]. Therefore, the evolution of floral organ identity genes, and flower evolution itself, can be understood in the context of MADS-box gene phylogeny. Almost all well-characterized plant MADS-box proteins share a conserved structural organization, called the “MIKC-type” structure, which includes MADS (M), intervening (I), keratin-like (K), and C-terminal (C) domains [25,26].

As angiosperm reproductive organs, flowers are under huge selective pressure and show a great diversity of characters in different plants. Stamines are defined as “sterilized stamens”, and have resulted from a dramatic evolutionary transformation of a stamen subset [27,28]. Zingiberaceae is a highly evolved monocotyledon with flowers that have strongly modified and degenerate androecia. Six stamens are divided into two whorls, in which four androecial members are represented by petaloid stamens, one is missing, and only one is fertile [29].

The genus *Alpinia* in Zingiberaceae is characterized by flexistylous styles that move during flowering [30]. *Alpinia* populations comprise two phenotypes, anaflexistylous and

cataflexistylous morphs, classified on the direction of stigma movement during flowering. Cataflexistylous flowers shed pollen in the morning and have stigmas exposed to pollinators in the afternoon, whereas anaflexistylous flowers shed pollen in the afternoon and have stigmas exposed to pollinators in the morning. The stigma positions of both types result from different stylar move directions. At around noon, the styles of cataflexistylous flowers begin to grow and curve downwards, whereas the styles of anaflexistylous flowers grow and curve upwards [30].

Morphological evolution always proceeds with changes in developmental processes. The aforementioned ABC model of flower developmental genetics opened a window on a better understanding of the homeotic changes in organ properties in the four floral whorls. In this context, it should also be interesting to understand the potential evolutionary transfer of properties between whorls [1,26,28]. We chose *Alpinia oblongifolia* as the model system with which to study the special floral structure of *Alpinia* (Zingiberaceae). To better understand the molecular mechanisms controlling floral development in the genus *Alpinia*, we explored B- and C-function genes in *A. oblongifolia*. We report the isolation, sequence, and expression analyses of two *PI*- and *AG*-like MADS-box genes that may be involved in petal, stamen, carpel, and ovule development in *A. oblongifolia*. These genes provide novel insights into the conservation and diversification of *PI*- and *AG*-like MADS-box genes in monocotyledonous plants.

2. Materials and methods

2.1. Plant material

Inflorescences of *A. oblongifolia* are produced from the shoot apical meristem, and are simple thyrses. The flowers of *A. oblongifolia* are zygomorphic; the perianth is differentiated into two whorls of three members each, and the sepals are united into a synsepalous calyx. The corolla tubes are slightly longer than the calyx, with three oblong lobes; the central lobe is usually wider than the lateral lobes. The labellum is ovate and white with two red stripes from the base to the middle, and the apex is two-lobed. The lip is formed by the two united lateral inner stamens (the median inner stamen is lost). Two small subulate lateral stamens are adnate to the base of the labellum. One fertile stamen bears two anthers. The stamen filament is firm, and the anther is large with a broad connective. The gynoecium is trilocular and inferior, with the style sticking out along the groove between the anthers. In contrast to the massive stamen, the hollow style is slender and weak. It is supported by the anther, which embraces it from above. In this way, the stigma is exactly above the anther. Other than the sepals and gynoecium, all floral members are united into a long floral tube [31] (Fig. 1).

Inflorescences of *A. oblongifolia* at different developmental stages were collected from the Mangao Nature Reserve of Xishuangbanna in Yunnan, southwest China. They were collected from late December to March, in the early flowering

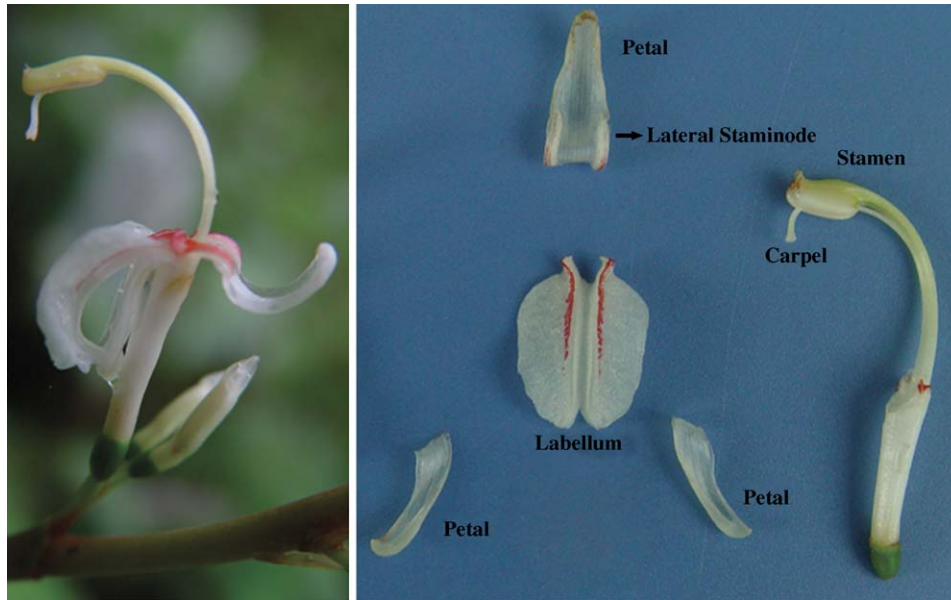


Fig. 1. The complete and dissected flower of *A. oblongifolia*.

season when floral meristems had already initiated and the floral organ primordia had begun to form.

2.2. Construction and screening of cDNA libraries

A cDNA library containing about 0.97×10^6 recombinants was constructed from developing *A. oblongifolia* inflorescences using the λ ZAP Cloning Kit (Stratagene). Total RNA was isolated from inflorescences using the Trizol method. Poly-A mRNA was then purified using the Oligotex[®] mRNA Midi Kit (Qiagen). cDNA was synthesized from 500 μ g of mRNA using the ZAP cDNA Synthesis Kit (Stratagene), according to the manufacturer's protocol. The library was packaged using the ZAP-cDNA Gigapack Gold Cloning Kit (Stratagene).

This *A. oblongifolia* cDNA library was screened with a ³²P-dCTP-labeled probe corresponding to the MADS domain of *A. hainanensis* AG- and PI-like MADS-box cDNAs. Their accession numbers in GenBank are [AY621155](#) and [AY621156](#), respectively [Song, unpublished].

Approximately 1.4×10^5 plaques from the inflorescence library were plated and transferred to Hybond N + membrane (Amersham). Prehybridization was performed in hybridization buffer ($5 \times$ standard saline citrate [SSC], 0.1% sodium dodecyl sulfate [SDS], and 0.1% sarkosyl) for 2 h at 55 °C. Hybridization was performed at moderate stringency at 55 °C overnight (about 12 h) with a MADS-box probe in hybridization buffer ($5 \times$ SSC, 0.1% SDS, and 0.1% sarkosyl), followed by three washes at 55 °C in $0.2 \times$ SSC and 0.1% SDS (15 min each). Filters were exposed to storage phosphor screens in an exposure cassette (Molecular Dynamics) overnight (about 12 h).

Putatively positive plaques were screened in second and third rounds at lower plaque densities. Independent putatively positive cDNA clones were rescued in pBluescript plasmid vector (Stratagene) by in vivo excision, according to the Stratagene protocol, to facilitate sequencing. Sequencing was

performed by the Shanghai BioAsia Biotechnology Co., Ltd. using an AB1 PRISM[™] 377 DNA sequencer (Perkin Elmer Applied Biosystems, Inc.).

2.3. Sequence analyses

Amino acid sequences deduced from the screened cDNAs were used for BLAST searches in the GenBank database (protein query–translated database) using the BLAST program at NCBI (<http://www.ncbi.nlm.nih.gov/blast>). Two MADS-box genes were identified repeatedly. Nucleotide sequences were translated to protein sequences using BioEdit version 7.0.0. For phylogenetic analyses, 34 types of PI- and AG-like MADS-box gene products were selected for comparison. The *Arabidopsis* A-function gene, *AtAP1*, and another type of B-function gene, *AtAP3*, are closely related to PI- and AG-like MADS-box genes in the MADS-box gene family. Therefore, they were used as outgroups. Sequence names were changed to include species initials where appropriate. The GenBank accession numbers of the amino acid sequences used are: *AtAP1* (Z16421), *AtAP3* (M86357), *AtPI* (D30807), *AtAGL1* (M55550), *AtAGL5* (M55553), *AtAGL11* (U20182), and *AtAG* (X53579) of *Ar. thaliana*; *LrGLOA* (AB071379) and *LrGLOB* (AB071380) of *Lilium regale*; *OsMADS2* (L37526), *OsMADS4* (L37527), and *OsMADS3* (L37528) of *O. sativa*; *TgGLO* (AB094967) of *Tulipa gesneriana*; *ZMM2* (X81200), *ZAG1* (L18924), *ZMM16* (AJ292959), *ZMM29* (AJ292961), and *ZMM18* (AJ292960) of *Zea mays*; *WPI1* (AB107991), *WPI2* (AB107992), and *WAG* (AB084577) of *Triticum aestivum*; *FBP1* (M91190), *FBP6* (X68675), *FBP7* (X81651), *FBP11* (X81852), *PMADS2* (X69947), and *PMADS3* (X72912) of *P. hybrida*; *NtGLO* (X67959) and *NAG1* (L23925) of *Nicotiana tabacum*; *TAG1* (L26295), *TAGL1* (AY098735), and *TAGL11* (AY098736) of *Lycopersicon esculentum*; *BAG1* (M99415) of *Brassica napus*; *PLENA* (S53900) of *An. majus*; *LIMADS2* (AY522502) of *L.*

longiflorum; and *AhAG* (AY621155) and *AhPI* (AY621156) of *Al. hainanensis*.

Alignments of two *A. oblongifolia* MADS-box amino acid sequences with those of 34 AG and PI homologues were initially compiled using the multiple sequence alignment program, ClustalX. The alignments were then refined by hand using BioEdit 7.0.0. The final amino acid alignment was adjusted (for NEXUS files). The N-terminal extensions that are present in many AG-like proteins were excluded from the alignments. The amino acid alignment was used for phylogenetic analyses, and to identify shared sequence characters and generally conserved motifs. Phylogenetic trees were constructed using maximum parsimony (MP) methods in PAUP* version 4.0b10 [32] on a Power Macintosh G4.

Maximum parsimony trees were generated with heuristic searches, and gaps were encoded as missing data. Multiple equal-length parsimony trees were collapsed into 50% majority rule consensus trees. Bootstrap values for all resolved nodes on the consensus trees were derived from the partition functions obtained after 100 replicates of MP analyses.

2.4. *In situ* hybridization

Tissue samples were fixed, embedded, sectioned, and hybridized using a modified version of the procedure described by Coen et al. [33], as used in the *Antirrhinum* laboratories of the Genetics Department, John Innes Centre, Norwich, United Kingdom.

The 510-bp *A. oblongifolia* *PISTILLATA* (*AoPI*) and 469-bp *A. oblongifolia* *AGAMOUS* (*AoAG*) fragments lacking the MADS-box were generated by polymerase chain reaction (PCR) and cloned into the pGEM-T Easy vector (Promega). Linear DNA templates (1 µg) were used to synthesize anti-sense and sense probes, which were labeled with the digoxigenin–UTP RNA labeling mix from Promega.

The probes were applied to 8 µm sections at a final concentration of about 10 ng/mL. Slides were photographed with a camera (Zeiss AxioCam HRc) mounted on a Zeiss Axioskop microscope (Zeiss Axioplan2). The photographic slides were scanned, digitized, and adjusted for contrast, brightness, and color balance with Adobe PhotoShop version 7.0.

3. Results and discussion

3.1. Cloning and sequence analyses of PI- and AG-like MADS-box genes from *A. oblongifolia*

To identify MADS-box gene activity in the reproductive organs of *A. oblongifolia*, we screened a cDNA library of *A. oblongifolia* with ³²P-dCTP-labeled probes made from the MADS domain of *A. hainanensis* AG- and PI-like MADS-box cDNAs. After all positively hybridizing clones were sequenced, two MADS-box-related clones were repeatedly identified. One clone was closely related in sequence to the B-class gene, *PI*, and was designated *AoPI*. Another clone was related to the C-class gene, *AG*, and was designated *AoAG*.

AoPI is 841 bp long including the poly-A tail instead of 826 bp long and encodes a 208 amino acid protein; *AoAG* is 971 bp long and encodes a 229 amino acid protein. The deduced amino acid sequences contain the conserved MADS domain, which is highly conserved among MADS proteins. They also have a K-box domain, which is less well conserved than the MADS domain.

Comparisons of the deduced *AoPI* and *AoAG* amino acid sequences with sequences of PI- and AG-like MADS-box proteins from *Arabidopsis* and from well-studied monocots such as rice, maize, and wheat showed that the amino acid sequence of *AoPI* is 52.8%–67.9% identical to that of the PI homologues (Fig. 2; Table 1). The amino acid sequence of *AoAG* is 60.0–65.9% identical to that of the AG homologues (Fig. 3; Table 2).

3.2. Phylogenetic analyses

Recently, the compilation of available MADS-domain sequences allowed the MADS-domain proteins to be classified into several distinct groups [25]. To look more closely at the relationships between members of the *PI* and *AG* gene groups, a phylogenetic tree of selected members of plant PI- and AG-like MADS-box proteins was generated. The cladogram is based on seven trees of equal length that contain 200 parsimony information characters (length 1544; consistency index = 0.6924; retention index = 0.8066; Fig. 4).

The phylogenetic tree shows that AG homologues form a highly supported clade (93% bootstrap proportion [BP]), and that B-function protein PI homologues and AP3 form another clade (79% BP). Sequences from monocots within each group form a monophyletic subclade, suggesting that there was just one PI- and AG-like gene in the last common ancestor of the monocots and eudicots. The *A. oblongifolia* gene products reported here fall well within the groups of PI- and AG-like proteins (Fig. 4).

Within the PI group, *AoPI* is classified into a monocot PI-type subclade, and is closely related to *AhPI* (*A. hainanensis*), *LrGLOB* (*L. regale*), *LrGLOA* (*L. regale*), and *TgGLO* (*T. gesneriana*). The sequences from members of the Poaceae constitute a well-supported subclade (95% BP) to the exclusion of proteins from Liliaceae and Zingiberaceae (Fig. 4). This suggests that the last common ancestor of Liliaceae, Zingiberaceae, and Poaceae also contained just one PI-like gene, and that some events that caused an increase in the number of monocot PI-like genes occurred independently in the lineages that led to the extant Liliaceae, Zingiberaceae, and Poaceae.

AG-group proteins were separated into C- and D-function clades, and the C-function clade included dicot and monocot subclades. This shows that *AoAG* is closer to the C-function AG-like proteins than it is to the D-function AG-like proteins. As a result, *AoAG* was classified into a monocot AG-type subclade. Within the clade of monocot AG-like proteins, *AoAG* and *AhAG* (*A. hainanensis*) constitute a well-supported subclade (92% BP) to the exclusion of proteins from Poaceae. The branch supporting WAG and ZMM2 has moderate bootstrap values (Fig. 4), suggesting that the last common

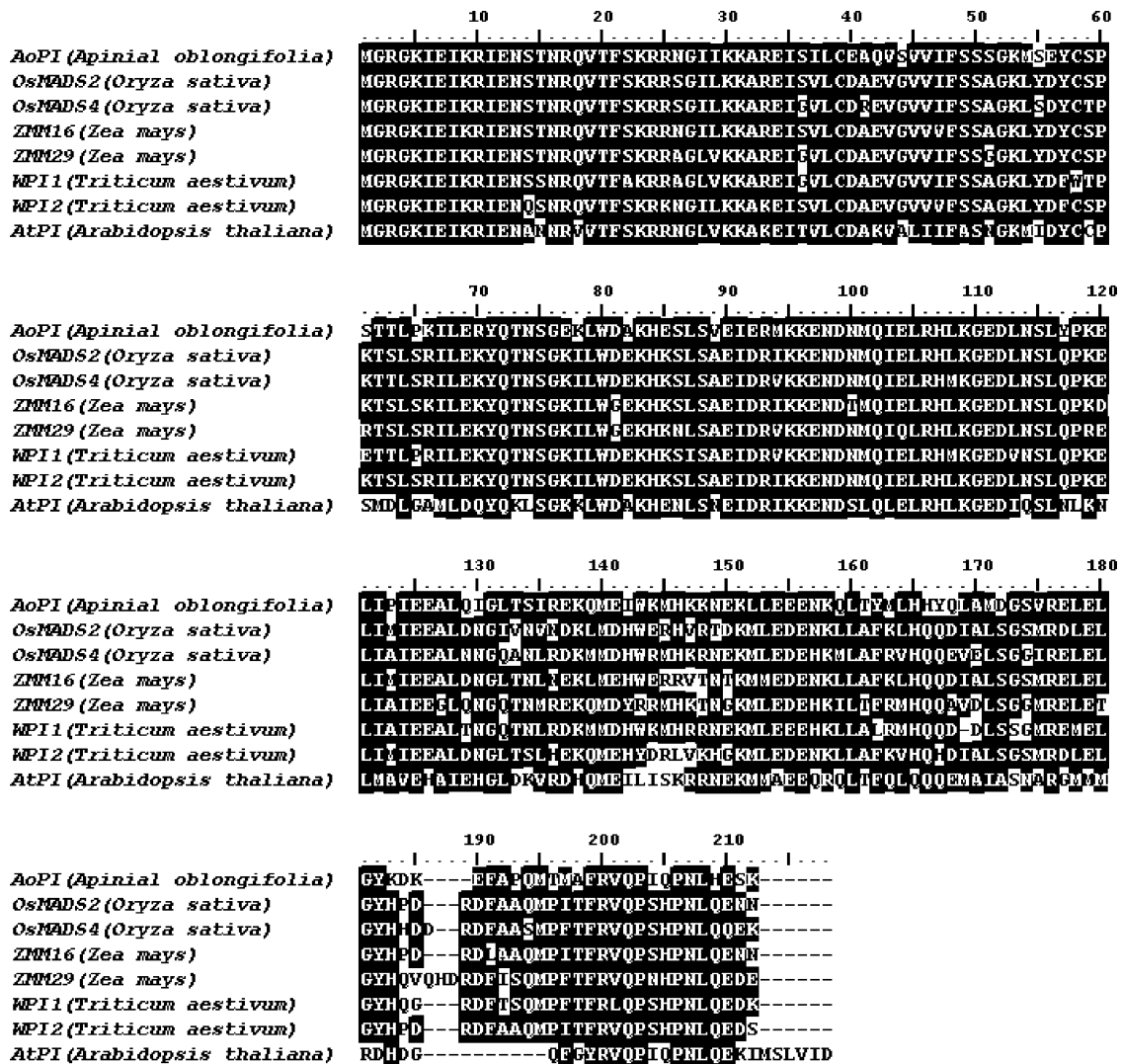


Fig. 2. An alignment of the complete amino acid sequence deduced from *AoPI* with those deduced from representative genes of the *PI* group from *A. thaliana* (*PI*), *O. sativa* (*OsMADS2* and *OsMADS4*), *Z. mays* (*ZMM16* and *ZMM29*), and *T. aestivum* (*WPI1* and *WPI2*). Amino acids conserved in at least four sequences are shaded, and dashes indicate gaps inserted into the sequence to optimize the alignment, which was generated using BioEdit version 7.0.0.

ancestor of Zingiberaceae and Poaceae also contained just one *AG*-like gene, and that some events that caused an increase in the number of monocot *AG*-like genes occurred independently in the lineages that led to extant Zingiberaceae and Poaceae.

Based on these results, *AoPI* and *AoAG* belong to the *PI* and *AG* groups, respectively, and are clearly separated from the proteins used as outgroups. With regard to the relationships within the groups of both *PI*- and *AG*-like genes, *AoPI* and *AoAG* are closely related to the monocot *PI* and *AG* groups, respectively. This provides clear evidence that *AoAG* is a homologue of *AG*, and that *AoPI* is a homologue of *PI*.

Table 1
Percentage amino acid identity of *PI*-like MADS-domain proteins (%)

	OsMADS2	OsMADS4	ZMM16	ZMM29	WPI1	WPI2	AtPI
AoPI protein	67.5	66.7	67.9	64.6	64.1	67.0	52.8
AoPI MADS-box	83.3	80.0	83.3	80.0	77.8	75.0	70.5

3.3. Floral development in *A. oblongifolia*

We used scanning electron microscopy (SEM) to outline the process of floral development in *A. oblongifolia*. Floral primordia are initiated at the axils of young bracts. At first, the floral apex is a long, transversely ellipsoidal protuberance, and it then becomes convex and flattens apically (Fig. 5A and B).

Sepals are initiated sequentially around the periphery of the floral primordia. In position, the three sepals are approximately 120° from each other (Fig. 5C–F). Following a short period of growth, the insertion sites of the sepals extend around the periphery of the flower until the margins of adjacent sepals become confluent to form the synsepalous calyx. However, the free tips of the sepals continue to enlarge to form a quincuncial aestivation, and finally cover the inner part of the flower (Fig. 5C–F).

During sepal initiation, the periphery of the floral promordium, interior to the sepals, enlarges to produce a raised ring primordium. The ring primordium is composed of

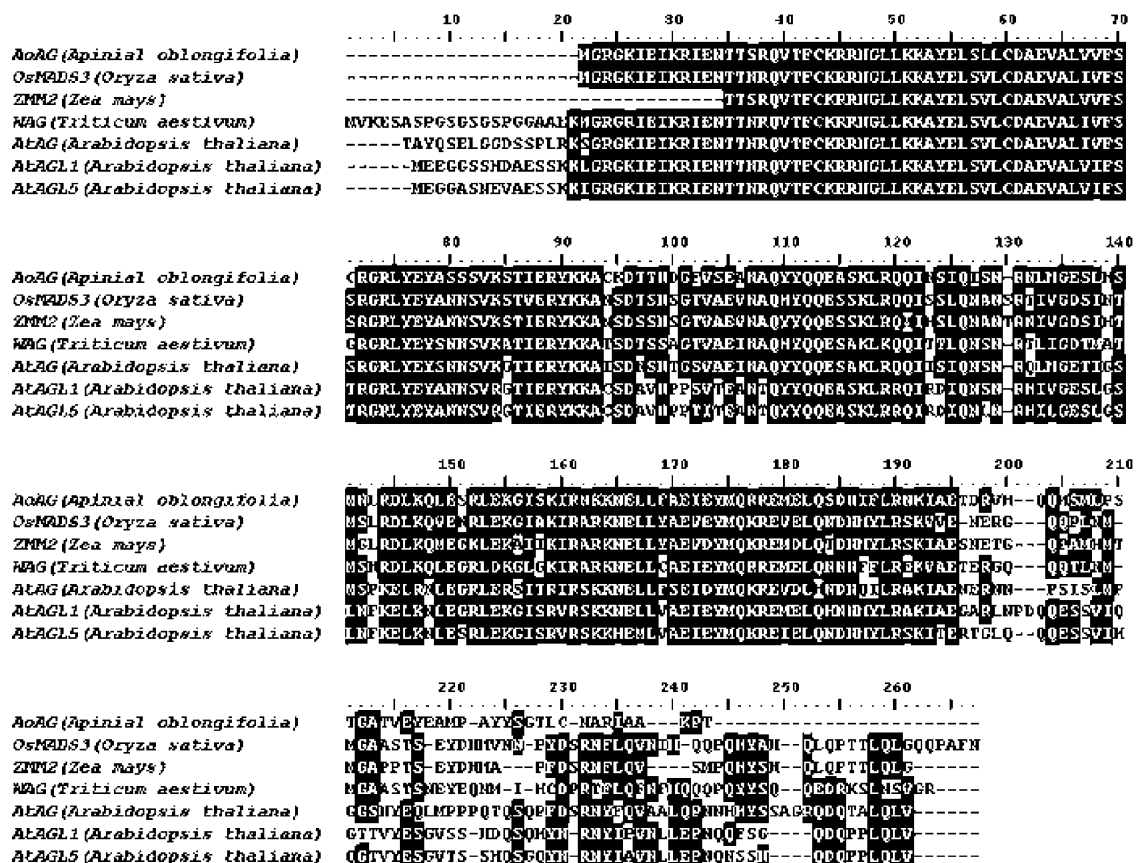


Fig. 3. An alignment of the complete amino acid sequence deduced from AoAG with those deduced from representative genes of the AG group from *A. thaliana* (AG, AGL1, and AGL5), *O. sativa* (OsMADS3), *Z. mays* (ZMM2), and *T. aestivum* (WAG). Amino acids conserved in at least four sequences are shaded, and dashes indicate gaps inserted into the sequence to optimize the alignment, which was generated using BioEdit version 7.0.0.

three slightly distinct common primordia, and assumes a triangle in cross-section (Fig. 5C). Before the sepals fuse at their base to form the synsepalous calyx, the ring primordium develops into three common primordia. These alternate with the sepals, from which both the petals and stamen form. From the early growth stages, the dorsal common primordium is slightly larger than the two ventral primordia, which are approximately equal in size. At later stages, the dorsal common primordium becomes distinctly larger. As a result of the growth of the common primordia, the center of the floral apex becomes sunken (Fig. 5D and E).

At a somewhat later stage, each common primordium divides transversely to produce a petal at the exterior and an inner androecial member (Fig. 5F). Separation of the three common primordia is sequential, beginning with the dorsal common primordium from which the fertile stamen and its associated petal are produced. The stamen consists of two pollen sacs (Fig. 5F). Separation of the two remaining common

primordia is nearly simultaneous. Each produces an exterior petal and an inner petaloid staminal member that will become the labellum (Fig. 5F and I).

At first, the petals and stamen primordia grow at equal rates, but soon the petals grow faster and cover the young bud entirely (Fig. 5G). The upper parts of the petals are free and have an imbricate aestivation.

As a result of the upward growth of the sepals and the common primordia of petal and stamen, the floral center becomes sunken. While the anthers form, the inception of the gynoecium begins centrally on the floral apex (Fig. 5H and I). The primordium of the carpel apex protrudes from the wall of the receptacle, and soon develops into a three-lobed mass. As the stamen enlarges, the thecae gradually surround the style until, at maturity, they completely enclose it.

According to the SEM micrographs, the floral development of *A. oblongifolia* is divided into several distinct stages: stage 1, the floral meristem appears as a hemispherical dome (Fig. 5A and B); stage 2, sepal primordia are initiated (Fig. 5C); stage 3, the sepals grow, while the three common primordia of the petals and stamens initiate (Fig. 5D and E); stage 4, the dorsal primordium splits transversely into a petal primordium and a stamen primordium, while each of the two ventral common primordia splits into a petal and a petaloid staminode that form the labellum at later stages (Fig. 5F). At about the

Table 2
Percentage amino acid identity of AG-like MADS-domain proteins (%)

	OsMADS3	ZMM2	WAG	AtAG	AtAGL1	AtAGL5
AoAG protein	65.3	62.6	60.0	65.5	65.9	65.2
AoAG MADS-box	93.1	93.2	96.0	91.2	86.1	91.4

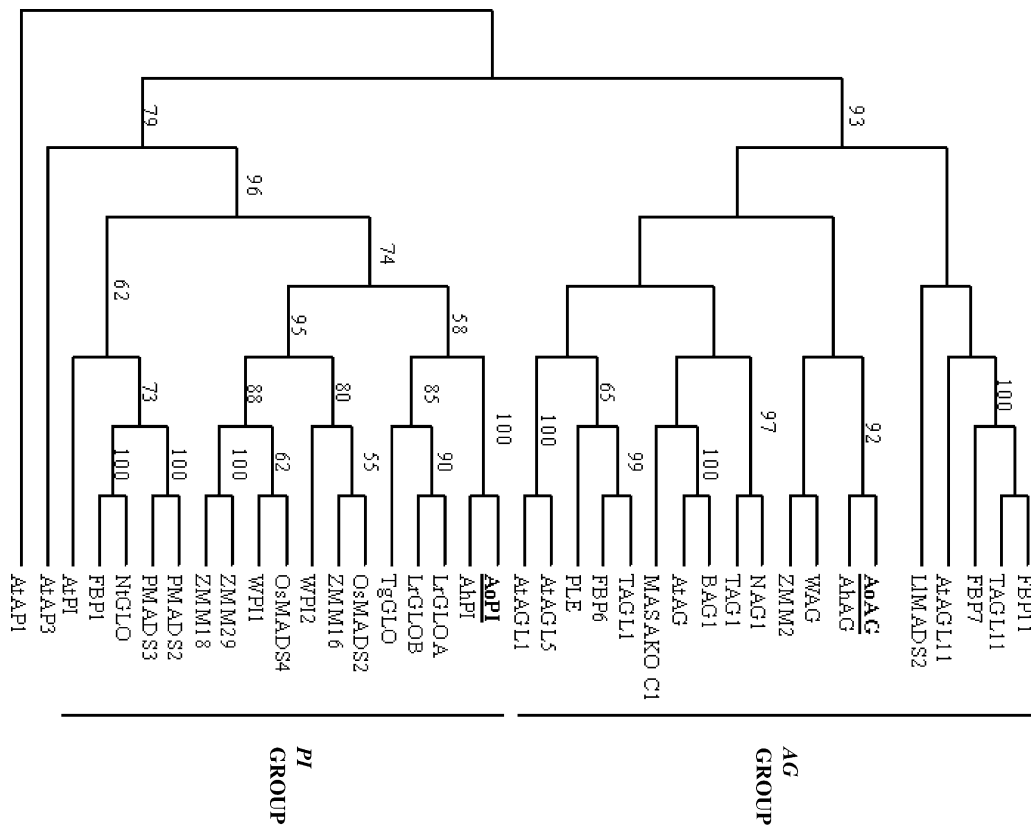


Fig. 4. Phylogenetic tree of selected members of the PI and AG MADS-box protein groups was constructed using MP methods in PAUP 4.0b10. Numbers above the internal branches give bootstrap probabilities of greater than 50. The proteins deduced from the cDNAs isolated in this study are shown in bold text and are underlined. Groups are labeled after an *Arabidopsis* representative of the respective clade, and are indicated by the bars on the right. *Arabidopsis* MADS-box proteins AP1 and AP3 were used as outgroups.

same time, sepals fuse into a tube. In stage 5, the synsepalous calyx grows and enfolds the flower, and the petals grow faster and cover the young bud entirely (Fig. 5G). When the calyxes and petals are removed, the gynoecium primordia are visible (Fig. 5H). At stage 6, the gynoecial primordia grow radially and fuse at the center of the ovary, and the labellum becomes visible (Fig. 5I).

3.4. Expression of *AoPI* and *AoAG* in *A. oblongifolia*

As shown by the RNA in situ hybridization experiments presented in Fig. 6, *AoPI* and *AoAG* were expressed on consecutive sections of the inflorescence at different developmental stages (Table 3).

At stages 1 and 2 of early floral development, *AoPI* was strongly expressed in the primordia from which the common primordium of stamen–dorsal petal, as well as the common primordia of labellum–lateral petal will initiate (Fig. 6A). The putative rice class B gene, *OsmADS2*, was not detected in early floral meristems before floral organ initiation. With the initiation and differentiation of the common primordia at stages 3 and 4, *AoPI* expression was maintained strongly in the stamen, petals, and labellum (Fig. 6B–D). With the development of carpels at stages 5 and 6, *AoPI* RNA was preferentially expressed in the anthers of the stamen and the labellum, and its expression in the petals decreased gradually (Fig. 6E and F).

Loss of expression began at the base of the petal and proceeded towards the tip. This tendency of higher expression in the stamen than in the petals was maintained into later developmental stages, when all floral organs were well differentiated (Fig. 6E and F). However, the expression of *OsmADS2* decreased rapidly and extensively in the stamen primordia in the late stages of floral development. Consequently, stronger expression was observed in the lodicules at that time [16]. cursory examination of the sections at all stages detected no expression above background in the sepals or gynoecia (Fig. 6A–F).

Sequence and phylogenetic analyses showed that *AoPI* is highly homologous to the B-function protein PI homologues of rice and maize. It also exhibits strong homology to PI isolated from *Arabidopsis*. Apart from some differences in detail, the observed localization of *AoPI* expression is consistent with the documented expression patterns of B-function genes such as *PI* (*Arabidopsis*) and *OsmADS2* (rice), which are expressed in the stamens and petals [14,20] (Fig. 6A–F). It appears that *AoPI* acts as a B-function PI protein in *A. oblongifolia*. The slight differences between *AoPI* and other PI-like genes may reflect the diversification of the PI-group genes in various plant species during evolution. However, the effects *AoPI* on transgenic *Arabidopsis* plants should be investigated to confirm whether it is functionally related to *Arabidopsis* PI.

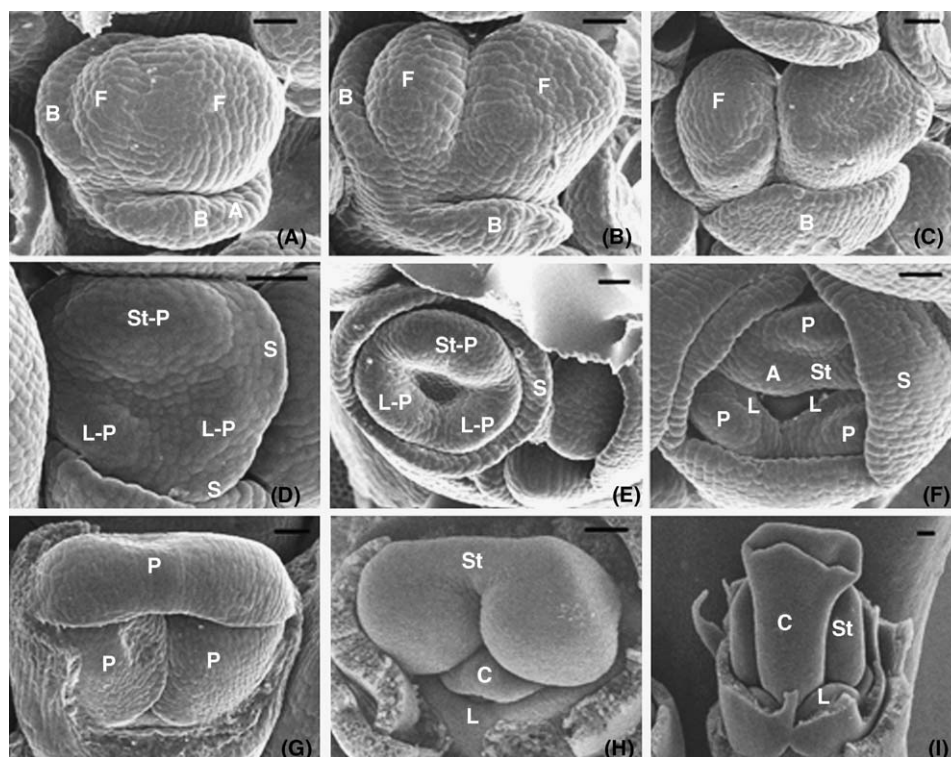


Fig. 5. (A–I) SEM micrographs of *A. oblongifolia* flowers. St-P, common primordium of stamen–dorsal petal; L-P, common primordium of labellum–lateral petal; F, floral primordium; B, bract; S, sepal; P, petal; A, anther; L, labellum; St, stamen; C, carpel. Scale bar = 50 μm .

Expression analyses using in situ hybridization showed that *AoAG* is expressed specifically in the stamen and carpels (Fig. 6; Table 3). This is also the case for *AG* [6,7]. However, the expression pattern of *AoAG* differs slightly from that observed for *AG*, which was detected uniformly in the carpels. Although *AoAG* mRNA was also detected in the stamen and ovules, only weak expression was observed in other parts of the carpels at early developmental stages (Fig. 6G, K, L). This result distinguishes *AoAG* from *AG*, suggesting that *AoAG* is more like the corresponding gene of rice.

Before the initiation of floral organ primordia at stage 1, *AoAG* was expressed at the center of the floral meristem from which androecium members (fertile stamen, lateral staminodes, and labellum) and carpels will initiate (Fig. 6G). However, expression of the C-function gene, *OsMADS3*, in rice was not detected in early flower meristems or young flowers. Strong expression of *OsMADS3* mRNA was first observed in the two inner whorls, where the stamens and pistils are formed [16]. With the initiation and differentiation of the common primordia in stages 3 and 4, *AoAG* was preferentially expressed in the stamen, and its expression in the carpel primordium was dispersive (Fig. 6H–J). *AoAG* was expressed in the labellum at stage 6, but it was not detected in the early developing staminodes at stage 4 (Fig. 6I and K). When the floral organs had formed at stages 5 and 6, *AoAG* mRNA was concentrated in the ovules and anthers, and had disappeared in the other parts of the carpels (Fig. 6J–L). Its expression in the labellum and filaments decreased gradually (Fig. 6J–L). A similar pattern of expression was reported for *OsMADS3* in the pistils. A low level of *OsMADS3* mRNA expression was observed in the

stamens and pistil primordia after the stamen primordia had initiated. A relatively strong signal was detected in the ovules at this stage [16]. Throughout the developmental stages, no expression above background was detected in the sepals or petals (Fig. 6G–L).

Other candidate *AoAG* homologues are genes such as *AGL1* and *AGL5* in *Arabidopsis*, which have been identified as members of the *AG* group. However, the expression of these genes is carpel-specific, because mRNAs for *AGL1* and *AGL5* were detected in particular regions of the gynoecium and ovules, whereas they were absent from stamens and other parts of the carpels [34,35]. In this way, they differ from *AoAG*. *AG* and its homologues reported to date are not only expressed in the fourth-whorl carpels, but also in the third-whorl stamens of the flowers [36–38]. Phylogenetic analyses clearly shows that *AoAG* is closer to *AG* than to *AGL1* or *AGL5* (Fig. 4). Moreover, *AoAG* is expressed not only in the carpels and ovules, but also in the stamen. We favor the assumption that *AoAG* is the putative *A. oblongifolia* C-functional gene that regulates stamen and carpel formation.

It appears likely that candidate class B and C genes in *A. oblongifolia* have maintained their ancestral functions and have not adopted derived functions. One possible explanation is that the slight differences between *AoAG*, *AoPI*, and other B- and C-functional genes reflect the diversification of the B- and C-group genes in various plant species during evolution. However, the potential effects conferred by as yet unidentified duplicate genes should be considered. Even if the developmental functions of these proteins in determining the identity of petaloid organs, stamens, and carpels are broadly conserved,

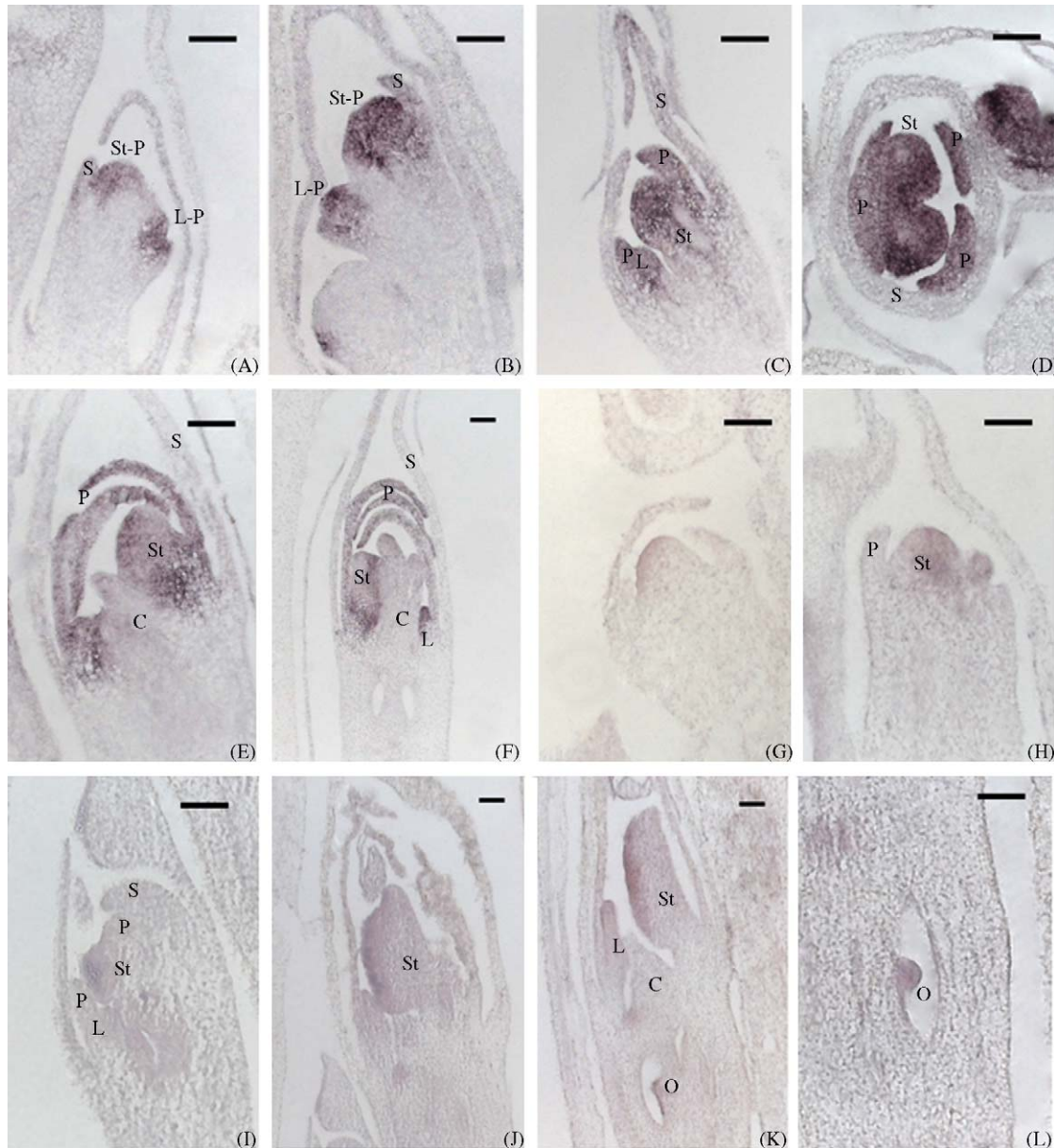


Fig. 6. In situ hybridization of *AoPI* and *AoAG* mRNAs in developing *A. oblongifolia* flowers. Developing inflorescences of *A. oblongifolia* were sectioned and hybridized with anti-sense mRNA probes for *AoPI* (A–F) and *AoAG* (G–L). A, B, G, and H are longitudinal flower bud sections. C, D, E, and I are longitudinal sections of immature flowers. F, J, K, and L are longitudinal sections of flowers with developed ovules. St-P, common primordium of stamen–dorsal petal; L-P, common primordium of labellum–lateral petal; S, sepal; P, petal; L, labellum; St, stamen; C, carpel; O, ovule. Scale bar = 50 μ m.

the exact parsing of ancestral functions among paralogs, together with possible instances of neofunctionalization, is likely to vary. Although *AG* is the only class C gene in *Arabidopsis*, two class C genes exist in tobacco [37,39], petunia

[38,40], cucumber [38,41], and maize [24,42]. Therefore, *AoPI* and *AoAG* may not be the only *PI*- and *AG*-like genes in *A. oblongifolia*. There may be other homologues of *PI* and *AG* produced by gene duplication events. It is reasonable to infer

Table 3
Expression of *AoPI* and *AoAG*

Floral development stage	Expression of <i>AoPI</i>	Expression of <i>AoAG</i>
Stage 1	Common primordia of stamen–petal and labellum–petal	Center of floral primordium
Stage 2	Common primordia of stamen–petal and labellum–petal	Stamen primordium
Stage 3	Common primordia of stamen–petal and labellum–petal	Stamen primordium
Stage 4	Petals, stamen, and staminodes	Stamen
Stage 5	Petals, stamen, and staminodes	Anthers
Stage 6	Petals, stamen, and labellum	Anthers, labellum, and ovules

that significant changes in the expression patterns of these genes would have occurred during evolution. Such changes partition the roles and restrict the functions of each gene product to a particular temporal range and/or region during floral development.

3.5. Labellum is derived from stamens in *A. oblongifolia*

The evolution of angiosperm floral diversity has been the subject of considerable study. It is widely accepted that whereas the stamens and carpels have each evolved only once, sterile organs have evolved many times within the angiosperms. However, details of these events remain unclear [28,43]. Petals are thought to have evolved independently in the core eudicots and monocots [28,43]. Much controversy has centered on the number and nature of petal derivation events within various angiosperm lineages. Petals derived from the stamens, the “andropetals”, have evolved many times within the lower eudicots, and at least once at the base of the higher eudicot and monocot clades. The second type of petal, the “bracteopetals”, derived from sepals or other sterile subtending organs [43].

Functional genes have possibly been formed by gene duplication and diversification events [26]. Previous studies have identified gene duplication events in *PI* and *AG* gene lineages at every phylogenetic level [44–46]. These gene duplications resulted in independent instances of paralog subfunctionalization and maintained functional redundancy. Multiple subfunctionalization events highlight the potential for gene duplications to increase morphological diversity [44–46]. In the current ABC model, because all stamens and carpels are homologous (that is to say, they have a common evolutionary origin), it is perhaps not surprising that the corresponding stamen and carpel identity genes should be homologues. The independent derivation events that gave rise to the different petal types of the angiosperms imply that petals in the core eudicots and monocots are not homologous organs. This may be reflected in the diversified structures and functions of the B and C group proteins. In the basal angiosperms, numerous duplications have occurred recently in the B lineage [44,45]. For example, a hypothesis has been proposed that duplications in the *AP3* and/or *PI* lineages in the Ranunculaceae family have played a role in the evolution of separate petal identity programs for the different types of petaloid organs [44]. Furthermore, according to the research of Kramer et al. [46], the functional homologues of the *AG* of *Arabidopsis* and *PLENA (PLE)* of *Antirrhinum* are representatives of separate paralogous lineages rather than simple genetic orthologs [46].

In this study, phylogenetic analyses of PI- and AG-like MADS-box proteins indicated that the PI- and AG-group genes are monophyletic. The PI-lineage genes are required for stamen identity, and the AG-lineage genes are required for stamen and carpel identity. This result confirms at the molecular level that stamens and carpels have a common evolutionary origin.

In *A. oblongifolia*, staminodes are highly petaloid structures [27,29,31] that have been genetically identified as stamens. During early growth stages, the *AoPI* gene is expressed strongly in the stamen and petals. In later developmental stages, the

expression of *AoPI* remains strong in the anthers and labellum, whereas it decreases in the petals and other parts of the stamen. This indicates that the stamen and labellum are similar. Expression of the C-class gene *AoAG* in the labellum is consistent with the inference that the labellum is derived from the stamen.

However, the relationship between MADS-box gene expression and staminode differentiation is still unclear. To better understand the mechanism of staminode differentiation in *A. oblongifolia*, additional work is required with transformants in which the floral structures are modified by B- and C-function genes. Did a shift in the expression of floral organ-identity genes result in the origin and diversity of staminodes in the Zingiberaceae? If so, this has important implications for the various roles of the floral homeotic genes in different species. Further study of the floral identity genes in other species of the Zingiberaceae is required to test this question.

Acknowledgments

We thank Dr. Da Luo for technical assistance, Dr. Wei Ma for helping to construct the cDNA library, Ms. Juan-Juan Song for providing *A. hainanensis* AG- and PI-like MADS-box cDNAs, Mr. Jiang-Yun Gao, Mr. Pan-Yu Ren, and Mr. Xiao-Bao Deng for their assistance in the collection of plant material, and Mr. Lang Li and Mr. Zhi-Ming Li for their help with the phylogenetic analyses, Ms. Ji-Jun Kong help with the work of floral development. We also thank Ms. Xiang-Ling Cao for her helpful discussion of some of the experiments. This research is supported by NSFC grant (30225007) and National Key Program for Basic Research of China (2001CCA00300) to Q.-J. Li.

References

- [1] P.K. Endress, Origins of flower morphology, *J. Exp. Zool. (Mol. Dev. Evol.)* 291 (2001) 105–115.
- [2] G. Theissen, Development of floral organ identity: stories from the MADS house, *Curr. Opin. Plant Biol.* 4 (2001) 75–85.
- [3] D.E. Soltis, P.S. Soltis, V.A. Albert, D.G. Oppenheimer, C.W. dePamphilis, H. Ma, M.W. Frohlich, G. Theissen, Missing links: the genetic architecture of flower and floral diversification, *Trends Plant Sci.* 7 (2002) 22–31.
- [4] J.L. Bowman, D.R. Smyth, E.M. Meyerowitz, Genetic interactions among floral homeotic genes of *Arabidopsis*, *Development* 112 (1991) 1–20.
- [5] Z. Schwarz-Sommer, P. Huijser, W. Nacken, H. Saedler, H. Sommer, Genetic control of flower development by homeotic genes in *Antirrhinum majus*, *Science* 250 (1990) 931–936.
- [6] E.S. Coen, E.M. Meyerowitz, The war of the whorls: genetic interactions controlling flower development, *Nature* 353 (1991) 31–37.
- [7] D. Weigel, E.M. Meyerowitz, The ABCs of floral homeotic genes, *Cell* 78 (1994) 203–209.
- [8] G.C. Angenent, L. Colombo, Molecular control of ovule development, *Trends Plant Sci.* 1 (1996) 228–232.
- [9] T. Honma, K. Goto, Complexes of MADS-box proteins are sufficient to convert leaves into floral organs, *Nature* 409 (2001) 525–529.
- [10] S. Pelaz, G.S. Ditta, E. Baumann, E. Wisman, M.F. Yanofsky, B and C floral organ identity functions require *SEPALLATA* MADS-box genes, *Nature* 405 (2000) 200–203.
- [11] M.A. Mandel, C. Gustafson-Brown, B. Savidge, M.F. Yanofsky, Molecular characterization of the *Arabidopsis* floral homeotic gene *APE-TAL1*, *Nature* 360 (1992) 273–277.

- [12] K.D. Jofuku, B.G.W. den Boer, M. Van Montagu, J.K. Okamoto, Control of *Arabidopsis* flower and seed development by the homeotic gene *APETALA2*, *Plant Cell* 6 (1994) 1211–1225.
- [13] T. Jack, L.L. Brockman, E.M. Meyerowitz, The homeotic gene *APETALA3* of *Arabidopsis thaliana* encodes a MADS box and is expressed in petals and stamens, *Cell* 68 (1992) 683–697.
- [14] K. Goto, E.M. Meyerowitz, Function and regulation of the *Arabidopsis* floral homeotic gene *PISTILLATA*, *Genes Dev.* 8 (1994) 1548–1560.
- [15] M.F. Yanofsky, H. Ma, J.L. Bowman, G.N. Drews, K.A. Feldmann, E.M. Meyerowitz, The protein encoded by the *Arabidopsis* homeotic gene *AGAMOUS* resembles transcription factors, *Nature* 346 (1990) 35–39.
- [16] J. Kyozuka, T. Kobayashi, M. Morita, K. Shimamoto, Spatially and temporally regulated expression of rice MADS-box genes with similarity to *Arabidopsis* class A, B and C genes, *Plant Cell Physiol.* 41 (2000) 710–718.
- [17] T. Münster, W. Deleu, L.U. Wingen, M. Ouzunova, J. Cacharrón, W. Faigl, S. Werth, J.T.T. Kim, H. Saedler, G. Theissen, Maize MADS-box genes *galore*, *Maydica* 47 (2002) 287–301.
- [18] A. Meguro, S. Takumi, Y. Ogihara, K. Murai, *WAG*, a wheat *AGAMOUS* homolog, is associated with development of pistillike stamens in alloplasmic wheats, *Sex. Plant Reprod.* 15 (2003) 221–230.
- [19] F. Fornara, L. Parenicová, G. Falasca, N. Pelucchi, S. Masiero, S. Ciannamea, Z. Lopez-Dee, M.M. Altamura, L. Colombo, M.M. Kater, Functional characterization of OsMADS18, a member of the AP1/SQUA subfamily of MADS-box genes, *Plant Physiol.* 135 (2004) 2207–2219.
- [20] Y.Y. Chung, S.R. Kim, H.G. Kang, Y.S. Noh, M.C. Park, D. Finkel, G. An, Characterization of two rice MADS-box genes homologous to *GLOBOSA*, *Plant Sci.* 109 (1995) 45–56.
- [21] H.G. Kang, J.S. Jeon, S. Lee, G. An, Identification of class B and class C floral organ identity genes from rice plants, *Plant Mol. Biol.* 38 (1998) 1021–1029.
- [22] B.A. Ambrose, D.R. Lerner, P. Ciceri, C.M. Padilla, M.F. Yanofsky, R.J. Schmidt, Molecular and genetic analyses of the *Silky1* gene reveal conservation in floral organ specification between eudicots and monocots, *Mol. Cell* 5 (2000) 569–579.
- [23] H.G. Kang, Y.S. Noh, Y.Y. Chung, M.A. Costa, K. An, G. An, Phenotypic alterations of petal and sepal by ectopic expression of a rice MADS-box gene in tobacco, *Plant Mol. Biol.* 29 (1995) 1–10.
- [24] M. Mena, B.A. Ambrose, R.B. Meeley, S.P. Briggs, M.F. Yanofsky, R.J. Schmidt, Diversification of C-function activity in maize flower development, *Science* 274 (1996) 1537–1540.
- [25] G. Theissen, J.T. Kim, H. Saedler, Classification and phylogeny of the MADS-box multigene family suggest defined roles of the MADS-box gene subfamilies in the morphological evolution of eukaryotes, *J. Mol. Evol.* 43 (1996) 484–516.
- [26] G. Theissen, A. Becker, A. Di Rosa, A. Kanno, J.T. Kim, T. Münster, K.U. Winter, H. Saedler, A short history of MADS-box genes in plants, *Plant Mol. Biol.* 42 (2000) 115–149.
- [27] J. Walker-Larsen, L.D. Harder, The evolution of staminodes in angiosperms: patterns of stamen reduction, loss, and functional re-invention, *Am. J. Bot.* 87 (2000) 1367–1384.
- [28] P.K. Endress, Floral structure and evolution of primitive angiosperms: recent advances, *Plant Syst. Evol.* 192 (1994) 79–97.
- [29] B.K. Kirchoff, Inflorescence and flower development in the hedycheiae (Zingiberaceae): *Scaphochlamys kunstler* (Baker) Holttum, *Int. J. Plant Sci.* 159 (1998) 261–274.
- [30] Q.J. Li, Z.F. Xu, W.J. Kress, Y.M. Xia, L. Zhang, X.B. Deng, J.Y. Gao, Z.L. Bai, Flexible style that encourages outcrossing, *Nature* 410 (2001) 432.
- [31] T.L. Wu, K. Larsen, Family Zingiberaceae, in: Z.Y. Wu, P.H. Raven (Eds.), *Flora of China*, vol. 24, Science Press, Beijing, China & Missouri Botanical Garden Press, St. Louis, Missouri, USA, 2000, pp. 342–343.
- [32] D.L. Swofford, PAUP*. Phylogenetic Analysis Using Parsimony. Version 4, Sinauer Associates, Sunderland, Massachusetts, USA, 2002.
- [33] E.S. Coen, J.M. Romero, S. Doyle, R. Elliott, G. Murphy, R. Carpenter, *Floricaula*: a homeotic gene required for flower development in *Antirrhinum majus*, *Cell* 63 (1990) 1311–1322.
- [34] B. Savidge, S.D. Rounsley, M.F. Yanofsky, Temporal relationship between the transcription of two *Arabidopsis* MADS-box genes and the floral organ identity genes, *Plant Cell* 7 (1995) 721–733.
- [35] C.A. Flanagan, Y. Hu, H. Ma, Specific expression of the *AGL1* MADS-box gene suggests regulatory function in *Arabidopsis* gynoecium and ovule development, *Plant J.* 10 (1996) 343–353.
- [36] Y. Mizukami, H. Ma, Ectopic expression of the floral homeotic gene *AGAMOUS* in transgenic *Arabidopsis* plants alters floral organ identity, *Cell* 71 (1992) 119–131.
- [37] S.A. Kempin, M.A. Mandel, M.F. Yanofsky, Conversion of perianth into reproductive organs by ectopic expression of the tobacco floral homeotic gene *NAG1*, *Plant Physiol.* 103 (1993) 1041–1046.
- [38] M.M. Kater, L. Colombo, J. Franken, M. Busscher, S. Masiero, M.M. Van, L. Campagne, G.C. Angenent, Multiple *AGAMOUS* homologs from cucumber and petunia differ in their ability to induce reproductive organ fate, *Plant Cell* 10 (1998) 171–182.
- [39] J.S. Zhang, Y.H. Wu, Q. Li, Y. Li, Molecular cloning and characterization of *NFBP6*, a putative floral homeotic gene, from tobacco, *Sex. Plant Reprod.* 11 (1998) 113–116.
- [40] S. Tsuchimoto, A.R. van der Krol, N.-H. Chua, Ectopic expression of *pMADS3* in transgenic petunia phenocopies the petunia *blind* mutant, *Plant Cell* 5 (1993) 843–853.
- [41] R. Perl-Treves, A. Kahana, N. Rosenman, Y. Xiang, L. Sil-berstein, Expression of multiple *AGAMOUS*-like genes in male and female flowers of cucumber (*Cucumis sativus* L.), *Plant Cell Physiol.* 39 (1998) 701–710.
- [42] G. Theissen, T. Strater, A. Fischer, H. Saedler, Structural characterization, chromosomal localization and phylogenetic evaluation of two pairs of *AGAMOUS*-like MADS-box genes from maize, *Gene* 156 (1995) 155–166.
- [43] A. Takhtajan, *Evolutionary Trends in Flowering Plants*, Columbia University Press, New York, 1991.
- [44] E.M. Kramer, V.S. Di Stilio, P.M. Schlüter, Complex patterns of gene duplication in the *APETALA3* and *PISTILLATA* lineages of the Ranunculaceae, *Int. J. Plant Sci.* 164 (2003) 1–11.
- [45] G.M. Stellari, M.A. Jaramillo, E.M. Kramer, Evolution of the *APETALA3* and *PISTILLATA* lineages of MADS-Box-containing genes in the basal angiosperms, *Mol. Biol. Evol.* 21 (2004) 506–519.
- [46] E.M. Kramer, M.A. Jaramillo, V.S. Di Stilio, Patterns of gene duplication and functional evolution during the diversification of the *AGAMOUS* subfamily of MADS Box Genes in angiosperms, *Genetics* 166 (2004) 1011–1023.